

Jean-Sébastien Blouin, Gunter P. Siegmund, Mark G. Carpenter and J. Timothy Inglis

J Neurophysiol 98:920-928, 2007. First published May 30, 2007; doi:10.1152/jn.00183.2007

You might find this additional information useful...

This article cites 32 articles, 7 of which you can access free at:

<http://jn.physiology.org/cgi/content/full/98/2/920#BIBL>

Updated information and services including high-resolution figures, can be found at:

<http://jn.physiology.org/cgi/content/full/98/2/920>

Additional material and information about *Journal of Neurophysiology* can be found at:

<http://www.the-aps.org/publications/jn>

This information is current as of August 6, 2008 .

Neural Control of Superficial and Deep Neck Muscles in Humans

Jean-Sébastien Blouin,^{1,2} Gunter P. Siegmund,^{1,3} Mark G. Carpenter,^{1,2,4} and J. Timothy Inglis^{1,2,4}

¹School of Human Kinetics and ²Brain Research Centre, University of British Columbia, Vancouver; ³MEA Forensic Engineers & Scientists, Richmond; and ⁴International Collaboration on Repair Discoveries, Vancouver, British Columbia, Canada

Submitted 17 February 2007; accepted in final form 26 May 2007

Blouin J-S, Siegmund GP, Carpenter MG, Inglis JT. Neural control of superficial and deep neck muscles in humans. *J Neurophysiol* 98: 920–928, 2007. First published May 30, 2007; doi:10.1152/jn.00183.2007. Human neck muscles have a complex multi-layered architecture. The role and neural control of these neck muscles were examined in nine seated subjects performing three series of isometric neck muscle contractions: 50-N contractions in eight fixed horizontal directions, 25-N contractions, and 50-N contractions, both with a continuously changing horizontal force direction. Activity in the left sternocleidomastoid, trapezius, levator scapulae, splenius capitis, semispinalis capitis, semispinalis cervicis, and multifidus muscles was measured with wire electrodes inserted at the C₄/C₅ level under ultrasound guidance. We hypothesized that deep and superficial neck muscles would function as postural and focal muscles, respectively, and would thus be controlled by different neural signals. To test these hypotheses, electromyographic (EMG) tuning curves and correlations in the temporal and frequency domains were computed. Three main results emerged from these analyses: EMG tuning curves from all muscles exhibited well-defined preferred directions of activation for the 50-N isometric forces, larger contractions (25 vs. 50 N) yielded more focused EMG tuning curves, and agonist neck muscles from all layers received a common neural drive in the range of 10–15 Hz. The current results demonstrate that all neck muscles can exhibit phasic activity during isometric neck muscle contractions. Similar oscillations in the EMG of neck muscles from different layers further suggest that neck motoneurons were activated by common neurons. The reticular formation appears a likely generator of the common drive to the neck motoneurons due to its widespread projections to different groups of neck motoneurons.

INTRODUCTION

The musculoskeletal anatomy of the human neck is complex: >20 pairs of superficial and deep muscles act on the cervical vertebrae and head to generate multidirectional forces and movements. Some neck muscles have similar lines of action (Vasavada et al. 2002) and therefore different muscles can conceivably be recruited to perform the same task. Despite this complexity and apparent redundancy, healthy individuals exhibit common patterns of activation for most neck muscles under isometric conditions (Gabriel et al. 2004; Keshner et al. 1989; Vasavada et al. 2002). A notable exception to this commonality is the splenius capitis muscle, which has demonstrated a consistent posterolateral directional preference in some studies (Gabriel et al. 2004; Vasavada et al. 2002) and a subject-specific anterolateral and/or posterolateral directional preference in others (Keshner et al. 1989; Mayoux-Benhamou et al. 1997). Although the role some neck muscles play in isometric force production has been documented, the physio-

logical synergies and neural control of the multi-layered neck muscles has received little attention.

The descending control of human neck muscles has only been studied in superficial muscles. During tonic contractions, Tijssen and colleagues observed synchrony in splenius capitis, sternocleidomastoid and levator scapulae at ~10–15 Hz in healthy individuals but reduced synchrony in patients with idiopathic torticollis (Tijssen et al. 2000, 2002). Because dystonic patients are believed to have deficits in sensorimotor integration, these authors hypothesized that the 10- to 15-Hz neck muscle oscillations could play a functional role in sensorimotor integration and be indicative of rhythmic olivary-cerebellar activity (Tijssen et al. 2000). Recent work by Grosse and Brown (2003) could present an alternate hypothesis for the origin of these oscillations in the superficial neck muscles. They identified in the deltoid muscles the presence of bilaterally synchronous 10- to 20-Hz muscular oscillations presumably representing reticulospinal activity. The presence and organization of these 10- to 15-Hz oscillations throughout the multiple layers of neck muscles have yet to be elucidated.

Deep and superficial axial muscles are thought to have different roles in stabilizing the spine and producing force or movement in humans. Based on their small moment arms and their attachments to adjacent vertebrae, the deep axial muscles (e.g., multifidus and intertransversus) are believed to stabilize the spine. With their large-moment arms and attachments to the skull and trunk, the more superficial muscles (e.g., trapezius and sternocleidomastoid) are believed to be predominantly prime movers. Recent evidence in humans partly supports these assumptions: activity in the deep cervical muscles was observed to be independent of the direction of cervical rotation (Bexander et al. 2005). These authors interpreted this result to mean that the cervical multifidus muscles were important for intervertebral control, a role similarly attributed to the multifidus muscles of the lumbar (Moseley et al. 2002) and thoracic (Lee et al. 2005) regions. These observations suggest that the deeper neck muscle layers stabilize adjacent vertebrae and could suggest that they receive descending neural control signals independent from the superficial neck muscles. On the other hand, the animal literature does not support such a dichotomy in the control of superficial and deep neck muscles. For example, single reticulo-spinal neurons are connected with different groups of neck motoneurons (Shinoda et al. 1996). In addition, all neck muscles recorded in cats and monkeys can exhibit phasic activity during voluntary and reflex activation (Corneil et al. 2001; Keshner et al. 1992). This difference between the animal and human literature is hard to reconcile,

Address for reprint requests and other correspondence: G. P. Siegmund, MEA Forensic Engineers & Scientists, 11-11151 Horseshoe Way, Richmond, BC V7A 4S5, Canada (E-mail: gunter.siegmund@meaforensic.com).

The costs of publication of this article were defrayed in part by the payment of page charges. The article must therefore be hereby marked "advertisement" in accordance with 18 U.S.C. Section 1734 solely to indicate this fact.

although it could be due to the limited number of intervertebral muscles recorded in animals. Because we recorded activity from human superficial and deep neck muscles, we expected the deep neck muscles would receive neural oscillations independent from those controlling the superficial muscle layers.

In the present study, we examined the hypothesis that deep and superficial neck muscles play different roles during isometric tasks in humans. To test this broad hypothesis, we used spatial, temporal and coherence patterns of EMG activity in deep and superficial neck muscles during different isometric tasks to examine three specific hypotheses: deep muscle activity would be uniform for all force directions (a postural role), whereas superficial muscle activity would be direction specific (a focal role); based on previous work, load would not influence the preferred direction or focus of muscle distributions (Keshner et al. 1989; Vasavada et al. 2002); and the neural signals controlling the deep neck muscles would not contain the previously observed 10- to 15-Hz oscillations but instead contain lower frequency oscillations because postural adjustments require mainly low-frequency corrections and the deep neck muscles contain a high proportion of slow-twitch (type I) muscle fibers (Boyd-Clark et al. 2001), which have a longer twitch rise-relaxation time than the fast-twitch muscle fibers (Jami et al. 1982).

METHODS

Subjects

Nine subjects (6M, 3F, 30 ± 6 yr) with no history of cervical injury, sensorimotor dysfunction or neck/back pain participated in the experiment. Subjects gave their written informed consent and were paid a nominal amount. The use of human subjects was approved by the UBC Clinical Research Ethics Board and conformed to the Declaration of Helsinki.

Imaging

All subjects underwent multiple magnetic resonance scans (Philips Gyroscan Intera 3.0 Tesla MRI scanner) to screen for existing pathology, to document neck muscle geometry, and to identify deep vasculature to avoid during wire insertions (Fig. 1B).

Instrumentation

EMG activity was measured using indwelling electrodes. Pairs of 0.05-mm wire (Stablohm 800A, California Fine Wire, Grover Beach,

CA) were inserted into the left sternocleidomastoid (SCM), trapezius (Trap), levator scapulae (LS), splenius capitis (SPL), semispinalis capitis (SsCap), semispinalis cervicis (SsCerv), and multifidus (Mult) muscles under ultrasound guidance (Sonos 5500, Agilent Technologies, Andover, MA). The electrodes, which had 1–2 mm of exposed wire and a 4-mm inter-electrode spacing, were designed to record multi-unit potentials from the neck muscles. All wire insertions were placed at the C_4/C_5 level (Fig. 1) with an additional multifidus insertion at the C_6/C_7 level. All wires were placed near the center of the muscle's horizontal cross section. In the SCM, the wire always remained superficial to the readily identifiable cleidomastoid subvolume (Kamibayashi and Richmond 1998). During wire extraction, ultrasound was again used to confirm the wire had not moved. Wire signals were amplified and band-pass filtered (30–1,000 Hz) using a Neurolog system (Digitimer, Welwyn Garden City, Hertfordshire, UK) before being digitized at 2 kHz. Isometric neck loads and moments were measured using a six-axis load cell (Bertec 4060H, ± 10 kN vertical, ± 5 kN horizontal, Worthington, OH; Fig. 1A).

Test procedures

Once instrumented, seated subjects performed three isometric tasks using their neck muscles: 50-N ramp and hold (R&H) in eight fixed directions (45° intervals), 25-N contractions with a continuously sweeping force direction, and 50-N contractions with a continuously sweeping force direction. The sweeping-force conditions consisted of a constant force amplitude applied in a slowly changing clockwise or counter-clockwise direction. Subjects had their head firmly clamped to an overhead load cell and their torso firmly strapped to a rigid seat back (Fig. 1A). This arrangement allowed subjects to apply an isometric force in any direction within a horizontal plane nominally at the height of their forehead and opisthocranium.

During the R&H task, subjects were asked to hold 50 N for 5 s in each of eight directions. Each direction was repeated twice and separated by rest periods of 30–60 s. Subjects received real-time visual feedback of their applied force direction and magnitude (a 2-dimensional plot of AP and ML reaction force) on a computer monitor. To assist the subjects, a “circular” area from 50 ± 5 N ranging $\pm 5^\circ$ of the target direction was drawn on the feedback screen. Ramp times were self-selected and typically took ~ 2 s.

After a rest period, subjects practiced applying a 25- and 50-N horizontal force against the load cell and slowly sweeping the direction of the applied force in the horizontal plane through 720° (2 complete rotations), beginning with extension. Depending on the force requirements, a 25- or 50-N circle was superimposed on the two-dimensional (2D) visual-feedback plot of AP and ML forces to assist subjects in maintaining the desired force level throughout the

TABLE 1. Mean focus (r) of the EMG tuning curves for the sweeping isometric contractions

Muscles	Condition				Repeated-Measures ANOVA		
	Counter-clockwise		Clockwise		Load	Direction	Interaction
	25 N	50 N	25 N	50 N			
1 SCM	0.22 \pm 0.10	0.36 \pm 0.15	0.20 \pm 0.12	0.30 \pm 0.15	$F = 37.45$	$P = 0.000$	
1 LS	0.37 \pm 0.20	0.53 \pm 0.13	0.43 \pm 0.12	0.53 \pm 0.09	$F = 21.77$	$P = 0.002$	
1 Trap	0.50 \pm 0.23	0.58 \pm 0.18	0.52 \pm 0.19	0.55 \pm 0.15			
1 SPL	0.28 \pm 0.17	0.29 \pm 0.11	0.32 \pm 0.13	0.29 \pm 0.16			
1 SsCap	0.44 \pm 0.20	0.55 \pm 0.16	0.43 \pm 0.21	0.54 \pm 0.18	$F = 13.17$	$P = 0.007$	
1 SsCerv	0.57 \pm 0.16	0.65 \pm 0.12	0.55 \pm 0.19	0.66 \pm 0.12	$F = 14.28$	$P = 0.005$	
1 Mult.C4	0.49 \pm 0.22	0.53 \pm 0.18	0.46 \pm 0.26*	0.58 \pm 0.18*	$F = 3.750$	$P = 0.089$	$F = 6.720$
1 Mult.C6	0.59 \pm 0.05	0.66 \pm 0.06	0.57 \pm 0.11	0.62 \pm 0.09	$F = 7.269$	$P = 0.031$	

Values are means \pm SD. The asterisks represent the values that were significantly different one from another after decomposition of the interaction for the MultC4 ($P < 0.05$). The italicized values represent main effects that were not significant but exhibited P values < 0.10 . Counter-clockwise and clockwise represent the directions of isometric force production. SCM, sternocleidomastoid; LS, levator scapulae; Trap, trapezius; SPL, splenius capitis; SsCap, semispinalis capitis; SsCerv, semispinalis cervicis; Mult, multifidus.

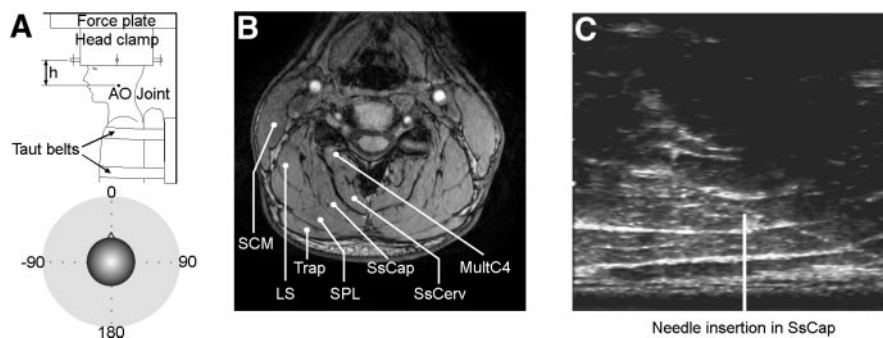


FIG. 1. Experimental setup and electrode placement. *A*: experimental setup illustrating the position of the head and trunk during the experiment. *Bottom*: bird's eye view of the subject's head and the angle corresponding to the direction of the exerted force (0°: flexion; ±180°: extension; -90°: left lateral flexion; 90°: right lateral flexion). *B*: transverse section of a magnetic resonance image at the level of C₄ illustrating the position of the various indwelling electrodes inserted. *C*: ultrasound image showing the reflection of the hypodermic needle during the insertion of the wires in the SsCap. SCM, sternocleidomastoid; LS, levator scapulae; Trap, trapezius; SPL, splenius capitis; SsCap, semispinalis capitis; SsCerv, semispinalis cervicis; Mult, multifidus.

entire sweep. Once able to perform the task smoothly, subjects performed two trials for each of four isometric sweep conditions—clockwise (+z) and counter-clockwise (-z) directions at both the 25- and 50-N levels—over a period of ~20 s/trial. The middle 360° (~10 s of data) from each trial were analyzed.

Data reduction

All EMG data were high-pass filtered (50 Hz) to remove artifacts. For each 50-N isometric contraction, a moving average was used to find the 500-ms interval of force minimizing variability (always <10%) of the required force (45–55 N). The RMS EMG for each muscle was then computed for the same interval. For the isometric sweep contractions, the average force and EMG were binned over 1° intervals. The RMS EMG for each 1° interval was computed and averaged over a moving 5° interval to generate continuous tuning curves. The binned force was also averaged over a moving 5° interval. To generate normalized tuning curves for each muscle, the RMS values from each direction (8 for the 50-N R&H task; 360 for the sweeping force tasks) were normalized by a muscle's maximum RMS value obtained during the 50-N R&H task.

Circular statistics were used to analyze the orientation (mean vector direction) and focus (a measure of distribution about the mean) of the EMG tuning curves for both the R&H and circular tasks (Batschelet 1981; Vasavada et al. 2002). EMG tuning curves for each muscle were computed by averaging both trials from each condition. Orientation (θ) was defined as the direction of the vector sum of an EMG tuning curve (8 vectors for R&H, 360 vectors for force sweeps). Focus (r) was computed by dividing the vector sum of the tuning curve by its arithmetic sum. Focus is thus bounded between 0 and 1, where 0 represent a uniform muscle distribution and 1 represents a muscle that operates in only one direction. Angular deviation (S) in radians was then computed using $S = (1 - r)^{1/2}$. To determine whether the EMG tuning curves were uniform, a Rayleigh test was performed (Batschelet 1981). Subsequently, a z -test for independent proportions was performed to compare the proportion of uniform versus nonuniform distributions observed in the superficial and deep neck muscle groups. The SCM, Trap, LS, SPL, and SsCap were classified as superficial neck muscles and the SsCerv, MultC4, and MultC6 as deep neck muscles. We chose the latter muscles to represent the deep neck muscles since they are intervertebral muscles. The orientation and focus of the EMG tuning curves for the force sweep tasks were also analyzed using a two-way repeated-measures ANOVA for load (25 and 50 N) and sweep direction (+z, -z). For all analyses, a significance level of $P < 0.05$ was chosen.

To identify potential agonist and antagonist muscles, Pearson correlation coefficients were computed between all pairs of indwelling RMS EMG computed during the 50-N force sweep tasks (+z and -z concatenated). To further examine the neural drive to the neck

muscles, the relative timing and coherence between pairs of neck muscles during the force sweep task were computed as follows. For each trial, raw EMG signals were full wave rectified and each signal's bias removed. Data for both force sweep directions (+z and -z) were concatenated for subject-by-subject and pooled-subjects analyses. The relative timing of the maximal correlation between muscle pairs recorded with indwelling electrodes was computed using cross-correlations of the subject-by-subject concatenated data. Common neural drive to pairs of muscles was analyzed using coherence of the pooled-subjects concatenated data. The auto-spectra, $f_{AA}(\lambda)$ and $f_{BB}(\lambda)$, and cross-spectrum, $f_{AB}(\lambda)$, were computed for each pair of muscles (λ denotes frequency). The spectra were estimated by averaging nonoverlapping windows of 1,024 points, and thus the frequency resolution of the spectra was 1.95 Hz. The components of the spectra at 0 Hz were not considered because of the concatenation methods. Coherence, $|R_{AB}(\lambda)|^2$, between the muscles was then computed using Eq. 1 (Halliday et al. 1995; Rosenberg et al. 1989). Coherence is a unitless measure bounded from 0 to 1, which indicates the linear relationship between two processes at various frequencies

$$|R_{AB}(\lambda)|^2 = \frac{|f_{AB}(\lambda)|^2}{f_{AA}(\lambda)f_{BB}(\lambda)} \quad (1)$$

We also computed the time-cumulant density estimates for all pairs of muscles recorded with the indwelling electrodes. The time-cumulant density function provides a time-domain representation of the correlation between signals. It estimates the timing and periodicity between synchronized inputs identified by the coherence estimates. We computed the time-cumulant density estimates using the inverse Fourier transform of the cross-spectrum, $f_{AB}(\lambda)$. Frequency-specific coherence and time cumulant density estimates were considered significant when they exceeded the 95% confidence interval computed according to Halliday et al. (1995).

RESULTS

Preferred direction of neck muscles

All subjects exhibited well-defined muscular activations when generating isometric forces in different directions (Fig. 2). All muscles exhibited preferred activation directions for the 50-N R&H task and the 50-N force sweep task (Rayleigh test, $P < 0.05$; Fig. 3). Only 5 of 184 muscle distributions in the 25-N force sweep task did not exhibit preferred activation directions (3 SCM, 1 SsCap, and 1 MultC4). The proportion of nonuniform distributions were similar between the superficial and deep neck muscles ($P > 0.05$). Between-subjects variability in preferred direction was minimal for most neck muscles

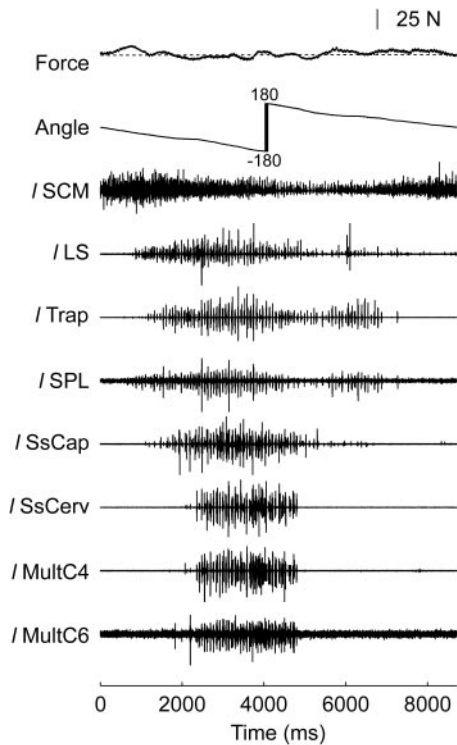


FIG. 2. Raw data from a single subject. Time series of the force and EMG data collected during a 50-N counter-clockwise continuous isometric contraction. The vertical scale bar represents 25 N. The abbreviations used for the neck muscles are listed in the caption of Fig. 1; l, left.

(typically <25°; Table 2). Even deep neck muscles, in particular the multifidus muscles (Fig. 4), exhibited good intersubject agreement with a posterolateral preferred direction of activity. The one exception was for the SPL muscle (Fig. 5): its preferred direction varied from posterolateral in four subjects, to lateral in one subject, to anterolateral in two subjects, to an alternation between posterolateral and lateral depending on the direction of the force production (clockwise vs. counter-clockwise) in two subjects.

In the force sweep task, preferred direction generally varied with sweep direction and focus generally increased with force amplitude (Fig. 3, Tables 1 and 2). Except for Trap and SPL, the preferred direction of the left neck muscles during clockwise sweeps was angled more posteriorly than for counter-clockwise sweeps (Table 2, Figs. 3–5). Trap and SPL were also the only two muscles that did not exhibit increased focus with increased force, although the focus of MultC4 increased only when tracing clockwise.

Neural control of neck muscles

The deep neck muscle layers (SsCap, SsCerv, MultC4, and MultC6) appeared to be synergists when performing the 50-N force sweep task (Fig. 6). Overall, the r^2 values between these muscles ranged from 0.22 to 0.90 with the greatest correlations observed between the SsCerv and MultC6 ($r^2 = 0.67$ – 0.89). Trap and LS were also correlated, with eight of nine subjects having r^2 values >0.2 (range: 0.01–0.76). Trap and LS muscle activity were correlated with activity in the deeper muscles (SsCap, SsCerv, MultC4, and MultC6; r^2 range: 0.01–0.81). On the other hand, the SPL showed a unique pattern of activity.

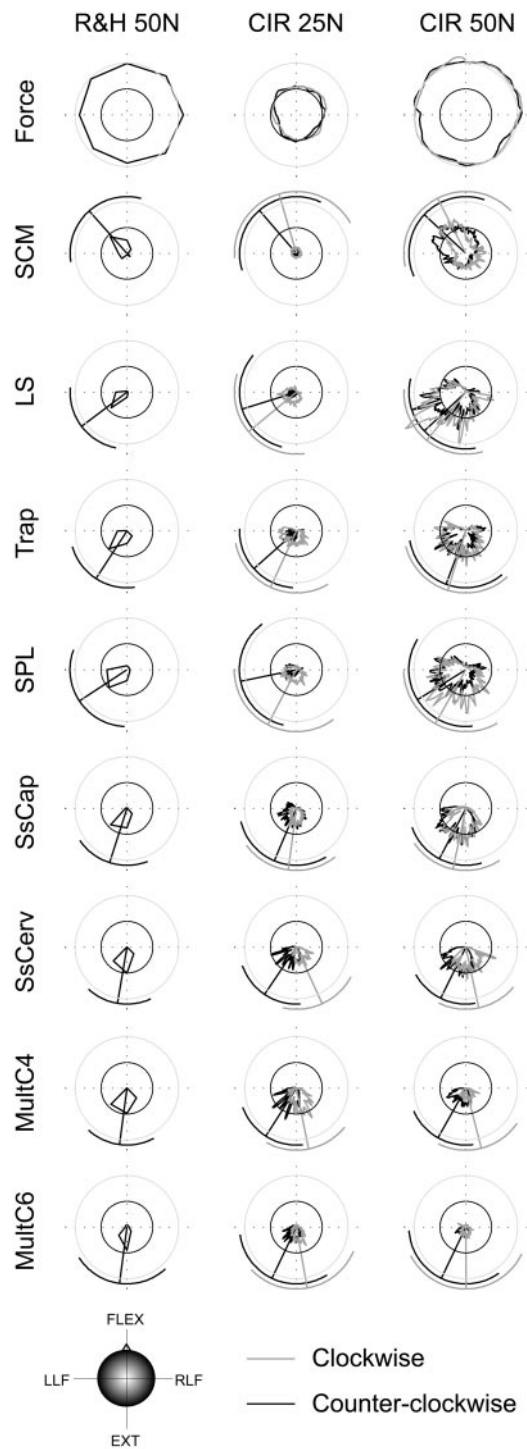


FIG. 3. Muscles tuning curves for a single subject. The black and gray lines originating from the center of the circle represent the mean resultant vector (preferred direction) of the muscle tuning curves, and the arcs illustrate the angular deviation of the resultant vectors. All EMG data has been normalized to the maximal EMG observed during the 50-N R&H task (dark circle in the polar plot). For the continuous isometric forces performed in the horizontal plane, the gray lines represent the clockwise rotations and the black lines the counter-clockwise rotations. The dark circle represents 25 N in the force plots and the maximal RMS EMG activity observed during the 50-N ramp-and-hold contractions in the muscle plots. The abbreviations used for the neck muscles are listed in the caption of Fig. 1; R&H, ramp and hold; CIR, circle; FLEX, flexion; EXT, extension; LLF, left lateral flexion; RLF, right lateral flexion.

TABLE 2. Mean preferred direction of the resulting vector for the EMG tuning curves during the sweeping isometric contractions

Muscles	Condition				Repeated-Measures ANOVA		
	Counter-clockwise		Clockwise		Load	Direction	Interaction
	25 N	50 N	25 N	50 N			
1 SCM	-49 ± 28	-43 ± 17	-66 ± 32	-51 ± 19	<i>F</i> = 3.63 <i>P</i> = 0.093	<i>F</i> = 6.597 <i>P</i> = 0.033	
1 LS	-109 ± 23	-114 ± 13	-130 ± 18	-130 ± 11		<i>F</i> = 5.948 <i>P</i> = 0.041	
1 Trap	-135 ± 40	-141 ± 24	-154 ± 20	-161 ± 23		<i>F</i> = 12.36 <i>P</i> = 0.008	
1 SPL	-102 ± 62	-97 ± 26	-130 ± 48	-117 ± 45		<i>F</i> = 3.816 <i>P</i> = 0.087	
1 SsCap	-147 ± 19	-144 ± 12	-171 ± 15	-168 ± 15		<i>F</i> = 18.74 <i>P</i> = 0.003	
1 SsCerv	-147 ± 7	-151 ± 8	-190 ± 9	-188 ± 8		<i>F</i> = 115.1 <i>P</i> = 0.000	
1 Mult.C4	-164 ± 20	-157 ± 13	-216 ± 46	-194 ± 13		<i>F</i> = 17.09 <i>P</i> = 0.003	
1 Mult.C6	-151 ± 11	-153 ± 13	-181 ± 21	-181 ± 12		<i>F</i> = 26.81 <i>P</i> = 0.001	

The italicized values represent main effects that were not significant but exhibited *P* values < 0.10. Counter-clockwise and clockwise represent the directions of isometric force production.

For some subjects, SPL activity correlated with the activity of the posterior muscles (*subjects 1 and 7*: $r^2 = 0.21$ and 0.79 , respectively) whereas for others, its activity correlated with the activity of SCM (Fig. 6; *subjects 5 and 8*: $r^2 = 0.43$ for both).

Muscle-muscle coherence analyses within subjects revealed a prominent peak in coherence between 10 and 20 Hz in muscle pairs with high r^2 coefficients (Fig. 7A; SsCap-MultC4). The cross-correlation and time cumulant distributions revealed similar features (Fig. 7, B and C). When the ~14-Hz peak in coherence was present, it was associated with cross-correlation lags and time cumulant peaks occurring within 25 ms of synchrony (0 lag). In addition, the cross-correlation and time cumulant distributions exhibited well-defined oscillations with a period of ~70 ms on both sides of

the peak value. The amplitude of these oscillations remained significant for three cycles (Fig. 7B), emphasizing the strength of the 14-Hz drive to the neck motoneurons. When averaged across subjects, the time lag between muscles was shortest between muscles of the deepest layers (SsCap, SsCerv, MultC4, and MultC6; range: 0.3–4.2 ms).

The time and frequency correlation analyses performed on the pooled-subjects data revealed the same general features. A significant peak in EMG-EMG coherence was observed around 10–15 Hz between pairs of agonist muscles (Fig. 8). This peak in coherence was easily identified in pairs of muscles showing high r^2 coefficient, e.g., between Trap and LS and between the deep neck muscles (SsCap, SsCerv, MultC4, and MultC6), but also between Trap and the deep neck muscles (*top left*, Fig. 8). The EMG-EMG muscle coherence was smallest for estimates involving the SCM or the SPL. These ~14-Hz synchronized neck muscles oscillations were accompanied by significant oscillations in the cumulant density peaking at ~0 ms and had a period of ~70 ms (*bottom right*, Fig. 8). Thus the between-muscle oscillations were synchronized and the ~14-Hz signal was again strong, as revealed by the 70-ms oscillations remaining significant for three to four cycles on both sides of the peak synchrony.

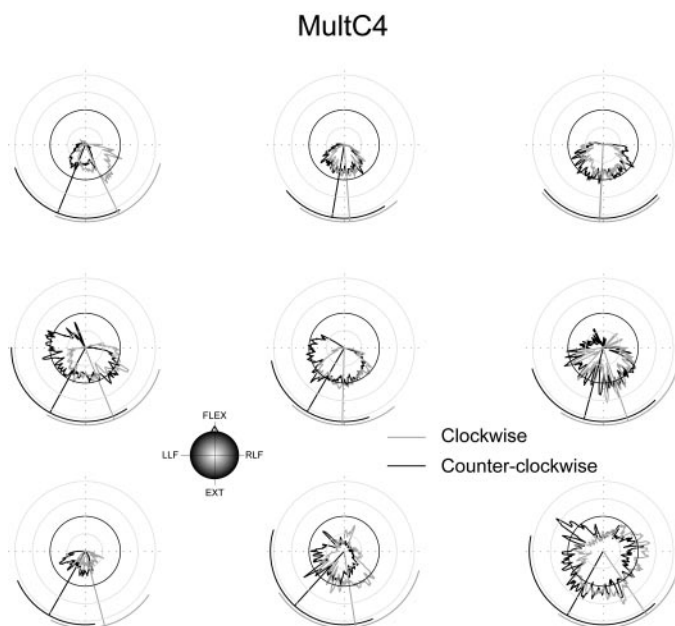


FIG. 4. Tuning curves for the multifidus muscle (measured at C₄) for all 9 subjects during the continuous circles isometric forces at 50 N. Each tuning curve represents the EMG data from a single subject. The black and gray lines originating from the center of the circle represent the mean resultant vector (preferred direction) of the muscle tuning curves and the arcs illustrate the angular deviation of the resultant vectors. The gray lines represent the clockwise rotations and the black lines the counter-clockwise rotations. All EMG data has been normalized to the maximal RMS EMG observed during the 50-N R&H task (dark circle in the polar plot). Note the consistent preferred posterolateral direction of the multifidus tuning curves for all subjects.

DISCUSSION

Our goal was to examine whether the superficial and deep neck muscles play different roles during isometric tasks. Our results showed well-defined tuning curves for all muscles tested, increased focus of most muscles with increased isometric force, and 10- to 15-Hz oscillations in the neural signals controlling the superficial and deep posterior neck muscles. Each of these findings is discussed in more detail in the following text, but from the perspective of our overall goal, these three findings disprove our three hypotheses, and we therefore reject the idea that superficial and deep neck muscles function differently from one another during isometric contractions.

Preferred direction and focus

All neck muscles studied exhibited well-defined preferred directions in their tuning curves for the 50-N isometric contractions. In addition, most muscles showed a similar preferred direction across all subjects. These observations suggest that

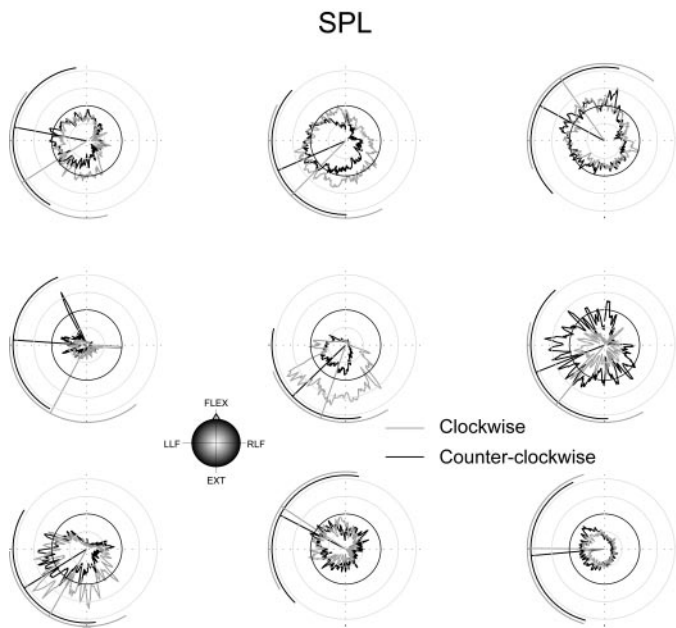


FIG. 5. Tuning curves for the SPL for all subjects during the continuous circles isometric forces at 50 N. Each tuning curve represents the EMG data from a single subject. The black and gray lines originating from the center of the circle represent the mean resultant vector (preferred direction) of the muscle tuning curves and the arcs illustrate the angular deviation of the resultant vectors. The gray lines represent the clockwise rotations and the black lines the counter-clockwise rotations. All EMG data has been normalized to the maximal RMS EMG observed during the 50-N R&H task (dark circle in the polar plot). Note the inconsistent preferred direction of the SPL tuning curves for all subjects.

the CNS copes with the anatomical complexity of the neck muscles by developing consistent muscle synergies to generate multidirectional patterns of force (Vasavada et al. 2002). The only exception to this rule was the SPL muscle, which showed variations in its tuning curves from anterolateral in some

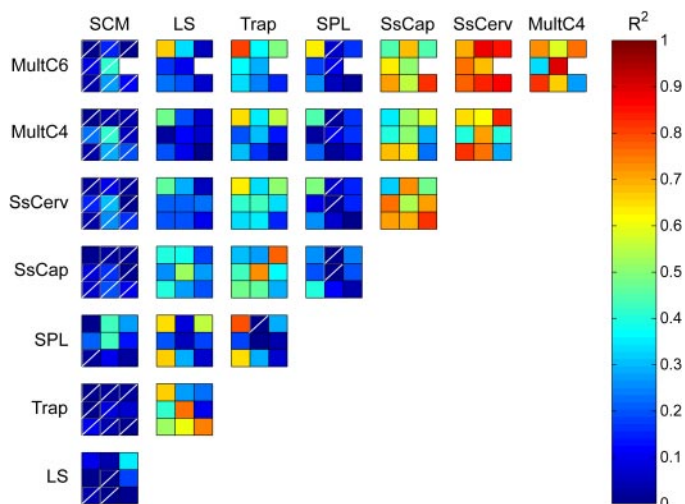


FIG. 6. Correlation between the muscle activities recorded from the various indwelling electrodes. The color gradient illustrates the amplitude of the Pearson's correlation coefficients (R^2). Each square of the 3×3 array represents the correlation from a single subject. The blank squares represent missing data for MultC6 in 1 subject. The white diagonal bar illustrates negative correlations. The correlation coefficients for the 3 deepest neck muscles were consistently high for all subjects. The abbreviations used for the neck muscles are listed in the caption of Fig. 1.

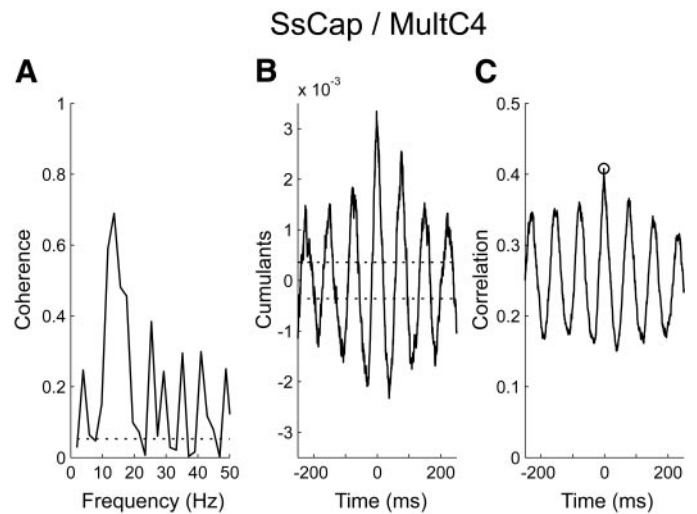


FIG. 7. Coherence, time cumulant and cross-correlation estimates between the SsCerv and cervical multifidus (MultC4) muscles for a single subject performing the 50-N continuous isometric contractions. The EMG data for the clockwise and counter-clockwise directions were concatenated. The dotted lines on the coherence and time cumulant density functions (A and B) represent the 0.95 confidence intervals. The circle on the cross-correlation illustrates the maximal correlation between muscles occurring near 0 ms. Note the significant peak in coherence between 10 and 20 Hz (A) and the similarity between the time cumulant estimates and the cross-correlation estimates (B and C).

subjects to posterolateral in others. Although our findings contradict the consistent posterolateral directional preference of SPL observed by some researchers (Gabriel et al. 2004; Vasavada et al. 2002), it replicates earlier observations of subject-specific anterolateral and/or posterolateral directional preferences (Keshner et al. 1989; Mayoux-Benhamou et al. 1997). This difference in SPL behavior is puzzling and could be related to electrode placement. We inserted our SPL wire electrode under ultrasound guidance at the C_4 level, whereas previous authors inserted their wires into SPL under the occipital protuberance where SPL can be manually palpated (Gabriel et al. 2004; Keshner et al. 1989; Mayoux-Benhamou et al. 1997; Vasavada et al. 2002). Another possible reason could be functional compartmentalization of the human SPL, similar to that described in the cat (Richmond et al. 1985; Wilson et al. 1983). Although careful attention was given to the identification of the neck muscles and insertion of the wires in all subjects, it is possible that the wires were in different functional compartments of SPL in different subjects.

SPL might also have a functional role during the multidirectional isometric neck muscle contractions that is distinct from the other neck muscles. Except for Trap and SPL, the neck muscle tuning curves were more focused when subjects generated larger forces (from 25 to 50 N). Because Trap is generally classified as a shoulder muscle and is innervated by the accessory nerve, a different modulation of its firing behavior compared with actual neck muscles is perhaps not surprising. The absence of an increase in SPL focus with increasing isometric force cannot be explained as simply. The large angular deviation of SPL could suggest that it acts to stabilize the head and neck rather than to apply focal forces during our task. It could also mean it behaves ambiguously when axial stabilization or motion is not required. Further work is needed to better understand the role of the SPL muscle.

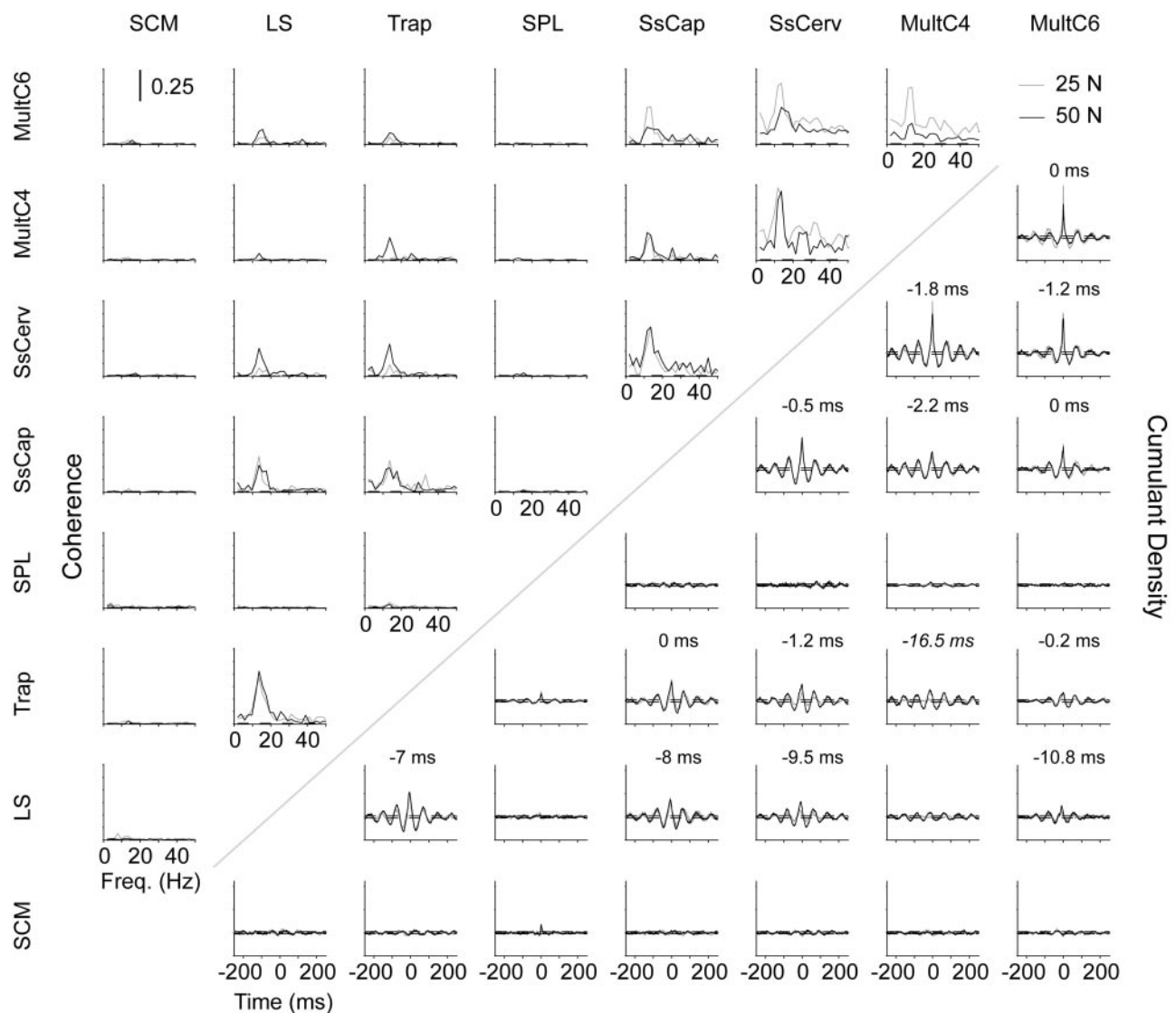


FIG. 8. Pooled coherence and time cumulant estimates for all subjects performing the 25- and 50-N continuous isometric contractions. The EMG data were concatenated for the clockwise and counter-clockwise directions. The dotted lines on the coherence and time cumulant density functions represent the 0.95 confidence intervals. The time (in ms) on the time-cumulant density functions represent the time lag at maximal correlation. Note the significant 10- to 15-Hz coherence for muscles showing good correlation (see Fig. 6) as well as the ~ 70 -ms oscillations in the corresponding time cumulant densities. The abbreviations used for the neck muscles are listed in the caption of Fig. 1.

The focused behavior of the cervical multifidus muscles during our multidirectional isometric tasks contradicts the idea that the cervical multifidus muscles have a unique role for intervertebral stabilization (Bexander et al. 2005). This is at odds with their role in the lumbar and thoracic regions (Lee et al. 2005; Moseley et al. 2002). Our results suggest that the Multi, SsCap, and SsCerv muscles act as agonists when applying forces in a well-defined arc of the multidirectional circle (posterolateral direction) and receive common neural signals to their motoneuron pool.

Neural control of the neck muscles in humans

Using multiple indwelling EMG recordings, we identified neck muscle synergies during multidirectional neck muscle contractions. The use of fine-wire electrodes to record the various neck muscles in the present experiment validates the observed correlations and excludes the confounder of EMG

cross-talk between muscles. This view is confirmed by the focused peak in coherence between 10 and 15 Hz, whereas coherence across the whole spectrum would be expected if cross-talk was present (Hansen et al. 2005).

Increased coherence in the 10- to 15-Hz bandwidth was observed both within the superficial and deep neck muscles and between the superficial and deep neck muscles. This observation contradicts our initial hypothesis that the superficial and deep neck muscles would receive different neural signals due to different functional roles. In addition, the time-domain correlation analyses revealed strong correlations occurring at ~ 0 - to 4-ms delays between the various muscles. This finding further supports the possibility that the various muscles received a common neural drive—delayed only by the peripheral conduction time. This neural drive was also characterized by recurring oscillations with a 70-ms period, arguing for strong 10- to 15-Hz descending signals. A close examination of the

raw EMG from the indwelling recordings reveals groups of motor units firing in a random order with ~ 70 -ms interspike intervals. These observations show that deep and superficial neck muscles acting as agonists are driven by a common neural drive during the production of continuous horizontal isometric force.

The frequency content of muscular oscillations can be used as a marker of the neural drive to the motoneurons (Baker et al. 1999; Hansen and Nielsen 2004; Kilner et al. 1999, 2003; Perez et al. 2006). For example, intermuscular and corticomuscular oscillations in the 16- to 35-Hz bandwidth have been linked to corticospinal drive to the limb motoneurons (Baker et al. 1999; Kilner et al. 1999). Neck muscular oscillations (SPL, SCM, and LS) in the 10- to 15-Hz bandwidth have been reported in healthy individuals performing tonic neck contractions (Tijssen et al. 2000, 2002). These authors hypothesized a functional role for these muscle oscillations in sensorimotor integration possibly through olivary-cerebellar rhythmic activity (Tijssen et al. 2000). Recently, Grosse and Brown (2003) observed synchronous bilateral muscle oscillations in the 10- to 20-Hz bandwidth induced by acoustic startle that were absent during voluntary activation and sham startle. They argued that coherence in the 10- to 20-Hz bandwidth could be used as a surrogate marker of reticulospinal activity because reticular structures are known to lie along the startle reflex pathway (Yeomans et al. 2002). The cat literature also provides compelling evidence that reticular neurons make monosynaptic excitatory connections with neck motoneurons (Iwamoto and Sasaki 1990; Sasaki 1999). These reticular neurons projecting to the neck motoneurons are known to be under cortical control (areas 4 and 6) (Alstermark et al. 1985; Isa and Sasaki 2002). In addition, single reticulospinal neurons are connected with different groups of neck motoneurons, suggesting the existence of motor primitives in the reticular formation to control neck muscle synergies (Shinoda et al. 1996). These characteristics of the reticulo-spinal neurons argue strongly for the involvement of reticulo-spinal activity in the generation of the 10- to 15-Hz neck muscular oscillations. Because our subjects performed voluntary contractions of the neck muscles that presumably involved cortical processing, we propose that the cortical activation of the neck motoneurons occurred through a relay in the reticular formation instead of a direct corticospinal projection to the neck motoneurons. This hypothesis is indirectly supported by the absence of 16- to 35-Hz oscillations in the neck muscles and by the weak monosynaptic corticospinal projections to the proximal versus distal musculature (Murayama et al. 2001).

In the present experiment, we did not observe 10- to 15-Hz synchronization between SPL and SCM (Fig. 8). Tijssen and colleagues, however, described motor synchronization in the 10–15 Hz for both the SCM and SPL (Tijssen et al. 2000, 2002). The apparent discrepancy between our results and those reported previously may be explained by the different tasks used in each experiment. Here, subjects were required to perform isometric neck muscle contractions in the horizontal plane, whereas Tijssen and colleagues asked their subjects to perform axial head rotations (Tijssen et al. 2000). During axial head rotation toward the right, the left SCM and right SPL act as synergists (Williams et al. 1995). There is no instance, however, in which the SCM and SPL act as synergists when performing multidirectional neck muscles contractions in the

horizontal plane. It appears that muscular synchrony between the various layers of neck muscles is present only when a combination of muscles act as synergists. From a functional perspective, it further suggests that common reticulospinal neurons drive the various neck motoneurons contributing to the desired motion or force, independently of the muscle layer. The presence of reticulospinal neurons projecting to different groups of neck motoneurons makes the reticular formation an ideal candidate to contain a detailed representation of neck motor synergies (Shinoda et al. 1996).

Load and focus

The greater focus we observed at the higher load contradicts previous work that showed the same or less focus at increased load (Keshner et al. 1989; Vasavada et al. 2002). Our method of a continuous force sweep in the horizontal plane provided better estimates of the focus than did the 8 or 16 discrete positions used in these earlier studies, and may explain the difference in results. Our results suggest that the complex anatomy of the neck muscles is well used by the CNS: when the load required of the neck muscles is low and numerous muscles can contribute to the required load in multiple directions, the nervous system effectively uses a combination of these muscles. As the load increased, the nervous system seems to recruit the muscles that can contribute specifically to generate the required load in a desired direction.

We performed a detailed analysis of the neck muscle activation and have shown that most muscles exhibit well-defined muscle tuning curves and preferred firing directions. Our analysis, however, was limited to the various layers of the posterior neck muscles and the SCM. The behavior of the deep neck flexor muscles was not studied and cannot be extrapolated from the current data set. We also confined our experiment to horizontal forces, and the condition of axial rotation or other head postures remains to be studied.

In conclusion, the present experiment showed that the various layers of neck muscles exhibited synchronized neural drive between 10 and 15 Hz. In addition, our results have shown that the neck multifidus muscles can exhibit phasic activity during multidirectional isometric contractions that is well correlated with the activity of the SsCap and SsCerv.

ACKNOWLEDGMENTS

We thank J. Nickel and M. Oala-Florescu of MEA Forensic Engineers and Scientists for help in building the equipment used for this experiment. Thanks also go to Dr. Alex Mackay at the UBC High Field MRI Centre for the MR scans and Dr. A. W. Sheel for the use of the ultrasound equipment (funded by Canada Foundation for Innovation).

GRANTS

This study was funded by grants from the Natural Sciences and Engineering Research Council to J. T. Inglis; the Canadian Institutes of Health Research, the Michael Smith Foundation for Health Research—BC Workers Compensation Board, and the Canadian Chiropractic Research Foundation to J.-S. Blouin; the British Columbia Neurotrauma Grant to J. T. Inglis, G. P. Siegmund, and J.-S. Blouin; and MEA Forensic Engineers & Scientists to G. P. Siegmund.

REFERENCES

- Alstermark B, Pinter MJ, Sasaki S. Pyramidal effects in dorsal neck motoneurons of the cat. *J Physiol* 363: 287–302, 1985.
- Baker SN, Kilner JM, Pinches EM, Lemon RN. The role of synchrony and oscillations in the motor output. *Exp Brain Res* 128: 109–117, 1999.

- Batschelet E.** *Circular Statistics in Biology*. London: Academic, 1981.
- Bexander CS, Mellor R, Hodges PW.** Effect of gaze direction on neck muscle activity during cervical rotation. *Exp Brain Res* 167: 3: 422–432, 2005.
- Boyd-Clark LC, Briggs CA, Galea MP.** Comparative histochemical composition of muscle fibers in a pre- and a postvertebral muscle of the cervical spine. *J Anat* 199: 709–716, 2001.
- Cornell BD, Olivier E, Richmond FJ, Loeb GE, Munoz DP.** Neck muscles in the rhesus monkey. II. Electromyographic patterns of activation underlying postures and movements. *J Neurophysiol* 86: 4: 1729–1749, 2001.
- Gabriel DA, Matsumoto JY, Davis DH, Currier BL, An KN.** Multidirectional neck strength and electromyographic activity for normal controls. *Clin Biomech* 19: 653–658, 2004.
- Grosse P, Brown P.** Acoustic startle evokes bilaterally synchronous oscillatory EMG activity in the healthy human. *J Neurophysiol* 90: 3: 1654–1661, 2003.
- Halliday DM, Rosenberg JR, Amjad AM, Breeze P, Conway BA, Farmer SF.** A framework for the analysis of mixed time series/point process data—theory and application to the study of physiological tremor, single motor unit discharges and electromyograms. *Prog Biophys Mol Biol* 64: 237–278, 1995.
- Hansen NL, Conway BA, Halliday DM, Hansen S, Pyndt HS, Biering-Sorensen F, Nielsen JB.** Reduction of common synaptic drive to ankle dorsiflexor motoneurons during walking in patients with spinal cord lesion. *J Neurophysiol* 94: 2: 934–942, 2005.
- Hansen NL, Nielsen JB.** The effect of transcranial magnetic stimulation and peripheral nerve stimulation on corticomuscular coherence in humans. *J Physiol* 561: 295–306, 2004.
- Isa T, Sasaki S.** Brainstem control of head movements during orienting: organization of the premotor circuits. *Prog Neurobiol* 66: 205–241, 2002.
- Iwamoto Y, Sasaki S.** Monosynaptic excitatory connexions of reticulospinal neurones in the nucleus reticularis pontis caudalis with dorsal neck motoneurons in the cat. *Exp Brain Res* 80: 277–289, 1990.
- Jami L, Murthy KS, Petit J, Zytnicki D.** Distribution of physiological types of motor units in the cat peroneus tertius muscle. *Exp Brain Res* 48: 177–184, 1982.
- Kamibayashi LK, Richmond FJ.** Morphometry of human neck muscles. *Spine* 23: 1314–1323, 1998.
- Keshner EA, Baker JF, Banovetz J, Peterson BW.** Patterns of neck muscle activation in cats during reflex and voluntary head movements. *Exp Brain Res* 88: 361–374, 1992.
- Keshner EA, Campbell D, Katz RT, Peterson BW.** Neck muscle activation patterns in humans during isometric head stabilization. *Exp Brain Res* 75: 335–344, 1989.
- Kilner JM, Baker SN, Salenius S, Jousmaki V, Hari R, Lemon RN.** Task-dependent modulation of 15–30 Hz coherence between rectified EMGs from human hand and forearm muscles. *J Physiol* 516: 559–570, 1999.
- Kilner JM, Salenius S, Baker SN, Jackson A, Hari R, Lemon RN.** Task-dependent modulations of cortical oscillatory activity in human subjects during a bimanual precision grip task. *Neuroimage* 18: 67–73, 2003.
- Lee LJ, Coppieters MW, Hodges PW.** Differential activation of the thoracic multifidus and longissimus thoracis during trunk rotation. *Spine* 30: 870–876, 2005.
- Mayoux-Benhamou MA, Revel M, Vallee C.** Selective electromyography of dorsal neck muscles in humans. *Exp Brain Res* 113: 353–360, 1997.
- Moseley GL, Hodges PW, Gandevia SC.** Deep and superficial fibers of the lumbar multifidus muscle are differentially active during voluntary arm movements. *Spine* 27: E29–36, 2002.
- Murayama N, Lin YY, Salenius S, Hari R.** Oscillatory interaction between human motor cortex and trunk muscles during isometric contraction. *Neuroimage* 14: 1206–1213, 2001.
- Perez MA, Lundbye-Jensen J, Nielsen JB.** Changes in corticospinal drive to dorsal motoneurons following visuo-motor skill learning in humans. *J Physiol* 573: 843–855, 2006.
- Richmond FJ, MacGillis DR, Scott DA.** Muscle-fiber compartmentalization in cat splenius muscles. *J Neurophysiol* 53: 868–885, 1985.
- Rosenberg JR, Amjad AM, Breeze P, Brillinger DR, Halliday DM.** The Fourier approach to the identification of functional coupling between neuronal spike trains. *Prog Biophys Mol Biol* 53: 1–31, 1989.
- Sasaki S.** Direct connection of the nucleus reticularis gigantocellularis neurons with neck motoneurons in cats. *Exp Brain Res* 128: 527–530, 1999.
- Shinoda Y, Kakei S, Muto N.** Morphology of single axons of tectospinal and reticulospinal neurons in the upper cervical spinal cord. *Prog Brain Res* 112: 71–84, 1996.
- Tijssen MA, Marsden JF, Brown P.** Frequency analysis of EMG activity in patients with idiopathic torticollis. *Brain* 123: 677–686, 2000.
- Tijssen MA, Munchau A, Marsden JF, Lees A, Bhatia KP, Brown P.** Descending control of muscles in patients with cervical dystonia. *Mov Disord* 17: 493–500, 2002.
- Vasavada AN, Peterson BW, Delp SL.** Three-dimensional spatial tuning of neck muscle activation in humans. *Exp Brain Res* 147: 437–448, 2002.
- Williams PL, Bannister LH, Berry MM, Collins P, Dyson M, Dussek JE, Ferguson MWJ.** *Gray's Anatomy* (38th ed.). New York, NY: Churchill Livingstone, 1995.
- Wilson VJ, Precht W, Dieringer N.** Responses of different compartments of cat's splenius muscle to optokinetic stimulation. *Exp Brain Res* 50: 153–156, 1983.
- Yeomans JS, Li L, Scott BW, Frankland PW.** Tactile, acoustic and vestibular systems sum to elicit the startle reflex. *Neurosci Biobehav Rev* 26: 1–11, 2002.